

Review

The Tyrrhenian Sea Circulation: A Review of Recent Work

Roberto Iacono *, Ernesto Napolitano, Massimiliano Palma and Gianmaria Sannino

National Agency for New Technologies, Energy and Sustainable Economic Development, C.R. Casaccia, 00123 Rome, Italy; ernesto.napolitano@enea.it (E.N.); massimiliano.palma@enea.it (M.P.); gianmaria.sannino@enea.it (G.S.)

* Correspondence: roberto.iacono@enea.it; Tel.: +39-06-3048-4790

Abstract: Knowledge about marine circulation and its variability is a basic requirement for the correct management of activities aimed at exploiting marine resources and for the prevention and eventual mitigation of the risks involved. The activities of the Marine Hazard Project, to which this special number of Sustainability is dedicated, focus on geothermal resources connected with some submerged volcanic systems located in the Tyrrhenian Sea. This sea hosts delicate coastal and marine ecosystems, and is characterized by rich dynamics, both driven by the interaction of the local forcing with the complex morphology and bathymetry of the basin, and by exchanges with adjacent sub-basins which take place at all depths. The main purpose of the present review is to summarize the present understanding of the Tyrrhenian Sea circulation and its variability, with special emphasis on the results of experimental and modelling works of the last decade.

Keywords: Tyrrhenian Sea circulation; Mediterranean Sea dynamics; deep circulation; seasonal variability; seamount effects; climate change



Citation: Iacono, R.; Napolitano, E.; Palma, M.; Sannino, G. The Tyrrhenian Sea Circulation: A Review of Recent Work. *Sustainability* **2021**, *13*, 6371. <https://doi.org/10.3390/su13116371>

Academic Editors: Mario Sprovieri, Salvatore Passaro, Alcide Giorgio di Sarra, Fabio Badalamenti and Fedra Francocci

Received: 16 April 2021

Accepted: 1 June 2021

Published: 3 June 2021

Publisher's Note: MDPI stays neutral with regard to jurisdictional claims in published maps and institutional affiliations.



Copyright: © 2021 by the authors. Licensee MDPI, Basel, Switzerland. This article is an open access article distributed under the terms and conditions of the Creative Commons Attribution (CC BY) license (<https://creativecommons.org/licenses/by/4.0/>).

1. Introduction

The coastal areas of the Tyrrhenian Sea—the main Italian sea, TYS hereafter—host delicate environments that are under pressure deriving from climate change and from the impacts of human activities. The latter may be amplified by local circulation features that can act as attractors of marine litter, or can disperse coastally released pollutants, endangering the local ecosystems, even in protected areas (see, e.g., the recent works [1,2], focusing on the Ligurian Sea, where the Pelagos Sanctuary for marine mammals is located). Detailed knowledge of marine circulation is therefore required for correct management of the socio-economic activities insisting on coastal areas, as well as for the planning of future activities aiming at the exploitation of marine resources, in order to understand, prevent, and eventually mitigate the risks involved. This needs to be achieved in the context of an evolving scenario, since important modifications of the hydrological properties of the TYS and, more generally, of the whole Mediterranean Sea, have been observed in the last few decades, whose impacts on circulation still need to be clarified (see, e.g., [3], about the Mediterranean surface warming trend, and [4], pointing out a strong increase of the salt content in the western Mediterranean since 2005).

The understanding of the TYS circulation is also hindered by the complex structure of the basin itself. The lower panel of Figure 1 displays the bathymetry of the TYS and shows its three main openings, the Corsica and Sardinia Channels (to the north and southwest, respectively), connecting the TYS to the westernmost part of the western Mediterranean, and the Sicily Strait (to the south), through which the western Mediterranean communicates with the eastern sub-basin, or Levantine basin. The TYS circulation is strongly affected by complex exchanges that take place at all depths through these openings, whose characterization has been—and still is—a key issue from an observational point of view. Smaller openings that strongly influence the surrounding circulation include the Bonifacio Strait, the narrow passage between Corsica and Sardinia, to the east of which a permanent

dipole is located (Bonifacio dipole, with the cyclonic pole to the north; see the yellow ovals in Figure 1), and the Messina Strait, between Sicily and the southern part of Italy, an area characterized by strong tidal currents. The red oval in Figure 1 highlights the region of the Palinuro Seamount, which is of direct interest for the Marine Hazard Project because of the hydrothermal systems present in the area, and of the associated mineral deposits (see [5], and references therein).

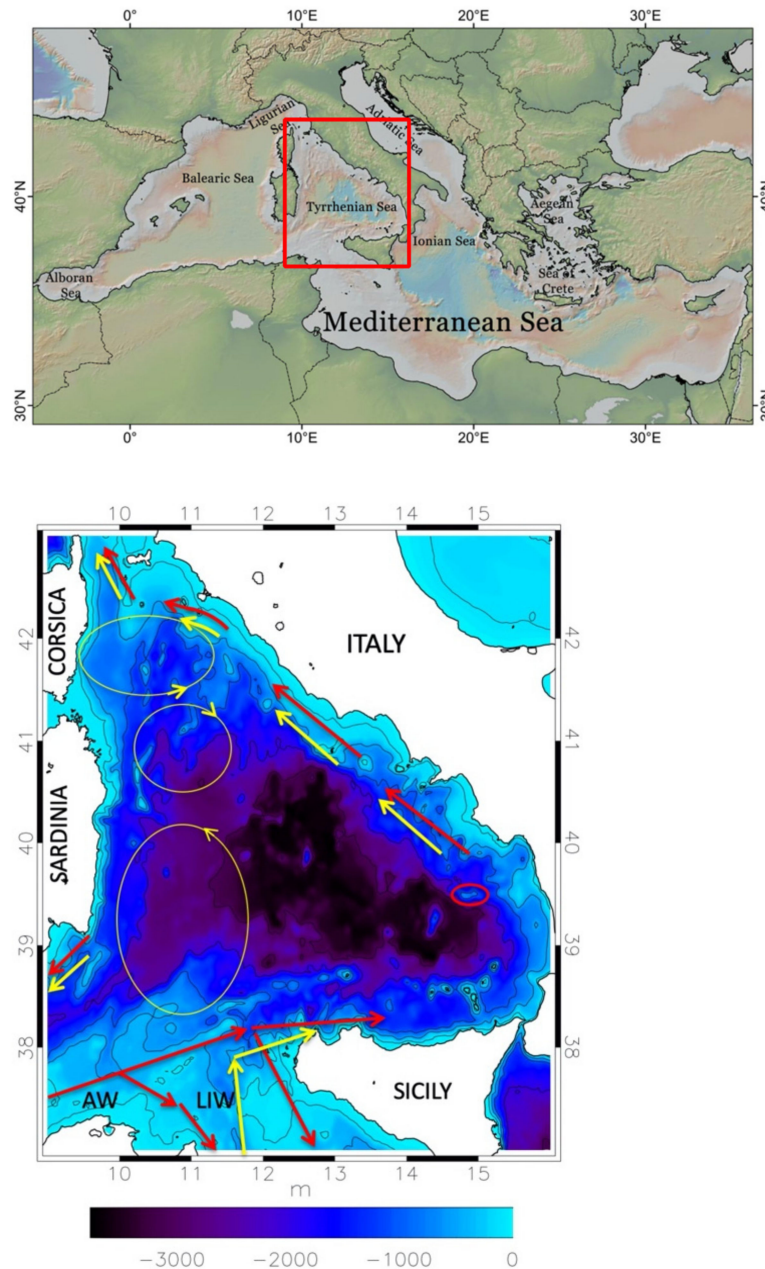


Figure 1. Top panel: the red box indicates the position of the Tyrrhenian Sea inside the Mediterranean basin. Lower panel: geometry and bathymetry (colours) of the Tyrrhenian Sea. The yellow ovals on the left schematically indicate three permanent structures of the basin circulation, the two poles of the Bonifacio dipole to the north, and a wide cyclonic area between Sardinia and Sicily. The arrows indicate the paths inside the basin of the Atlantic Water (AW; red) entering from the Sardinia Channel, and of the Levantine Intermediate Water (LIW; yellow) that enters from the Sicily Strait. The small red oval encompasses the Palinuro Seamount, to the southwest of which the Marsili Seamount can be recognized.

The hydrology and the dynamics of the TYS have been studied for a long time, and the large-scale picture resulting from the experimental campaigns of the 20th century has been summarized in several classical works [6–9]. In the present review, we mostly focus on the main developments from the last decade, which have led to a more detailed description of the TYS circulation and of its variability. For a short synopsis of previous investigations, the reader can refer to the introduction of [10], a paper that assesses the variability of the TYS surface circulation, mostly based on the analysis of satellite altimeter data. The synopsis includes some interesting works [11,12] in which simplified, barotropic models of the dynamics were used to study the relation between the structure of the large-scale circulation and that of wind-forcing, and numerical investigations performed with the first, relatively coarse-resolution, general circulation models (GCMs) implemented over the Mediterranean Sea [13,14].

During the 1990s, the observation landscape was enriched by the advent of systematic satellite measurements, revealing rich mesoscale dynamics that could not be adequately resolved by the aforementioned GCMs [15]. This has allowed for the construction of archives of several ocean physical parameters, such as the sea surface temperature (SST), the absolute dynamic topography (ADT; derived from altimeter measurements), with the associated reconstruction of the geostrophic circulation, and the turbidity, with spatial details going from about 1 km for the latter to about 14 km ($1/8^\circ$) for the altimeter data.

In the last decade, the use of these datasets in the Mediterranean context has increased (see [10,16,17], among others). The analysis of the altimeter and SST data has provided key insights about the structure of the circulation and its variability, which takes place on a variety of time-scales, ranging from seasonal to interannual, and to even longer scales associated with the global thermohaline cell of the Mediterranean. The observed interannual variability can be related to the atmospheric variability, but may also be an expression of internal, sub-basin dynamics (e.g., the NIG oscillation taking place in the northern portion of the Ionian Sea; see [18], and references therein).

These observations, however, only give information about the sea surface (SST), or the first few tens of meters of the water column (turbidity), or, in the case of altimeter data, about the surface layer. The latter extends from the sea surface down to the pycnocline, the narrow layer characterized by a strong density gradient that separates the surface water of Atlantic origin (Atlantic water, AW; upper 150 m), from the underlying intermediate water, which originates in the Levantine basin.

The satellite measurements are part of a large archive managed since 2015 by the European Copernicus Programme (for the sea, the Copernicus Marine Environment Monitoring Service; CMEMS), which includes both remote and In Situ observations. Useful information on the surface and intermediate layers, until depths of 700–800 m, is also provided by other observation programs, such as the temperature measurements by XBTs (eXpendable BathyThermographs) carried out by opportunity ships on some commercial sea lanes [19], and the surface drifter and profiling float measurements made by OGS (National Institute of Oceanography and Applied Geophysics), in the context of ARGO-ITALY [20]. Observations of the deepest layers are unfortunately rarer.

In this review, we discuss the picture of the TYS circulation that has emerged from these observations and recent numerical investigations, with particular attention to the south-eastern part of the basin. The water masses present in the TYS are described in Section 2, whereas Section 3 is devoted to the structure and seasonal variability of the TYS surface circulation, including results from recent works on coastal dynamics that have mostly focused on the waters facing Campania, the Italian region including the Gulf of Naples. The current understanding of the circulation in the intermediate and deep layers of the TYS—though still limited—is summarized in Section 4. Section 5 is concerned with the long-term variability of the properties of the TYS water masses, and Section 6 highlights some circulation effects due to the presence of localized topographic features. Conclusions are drawn in Section 7.

2. The Tyrrhenian Water Masses

From a hydrological point of view, the TYS is characterized by the presence of three main water masses: the AW, the LIW, and the WMDW. The AW, formerly denoted as Modified Atlantic Water (MAW), before the Mediterranean Science Commission (CIESM), in 2001, established the official acronyms currently used, and forms the surface layer (0–150 m). The Levantine Intermediate Water (LIW) occupies the layer between 200 m and 700 m of depth, whereas the Western Mediterranean Deep Water (WMDW) goes from about 1000 m of depth to the bottom. Besides these main water masses, there is also the Tyrrhenian Intermediate Water (TIW), which is located between the AW and the LIW, and the Tyrrhenian Deep Water (TDW), which is found in the range between 700 m and 1500 m of depth. Temperature salinity (TS) diagrams, obtained from Argo data covering the period 2004–2017, are shown in Figure 2, where red circles highlight the different water masses, characterized by distinctive hydrological signatures (similar diagrams were presented in [21]).

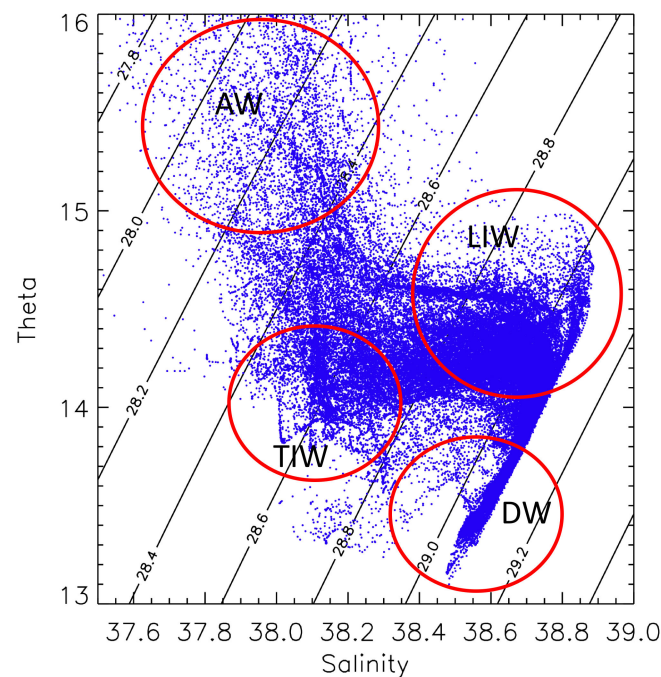


Figure 2. Temperature-salinity (T-S) diagram for the Tyrrhenian Sea, obtained from Argo measurements covering the period 2004–2017 (T in °C, S in psu). The red circles highlight the regions occupied by the main water masses. TIW and DW denote the Tyrrhenian Intermediate Water and the Deep Water, respectively.

2.1. Surface and Intermediate Waters

The surface water mass of the TYS is identified by the minimum salinity, and results from the inflow of AW in the south-western part of the Mediterranean basin, through the Gibraltar Strait. The horizontal distribution of salinity in this layer is characterized by a strong meridional gradient, with values ranging from about 36.2 psu in the southern region, in the Sardinia Channel, to 38.2–38.4 psu in the northern part of the TYS, in the region of the Bonifacio dipole, where important processes of vertical mixing take place. This distribution also exhibits a marked seasonal cycle, which we will discuss later in the paper.

The intermediate water masses, the LIW and the TIW, have different origins, because the first comes from the Levantine basin, and enters the TYS through the Sicily Channel (see the yellow arrows in the scheme of Figure 1), whereas the second is of local origin, as it has been conclusively shown in [21]. The TIW is found between the AW and the LIW, in the range 100–200 m, and is characterized by a local temperature minimum, whereas the LIW occupies a deeper and wider layer (200–700 m), and is characterized by local maxima

of temperature and salinity in the TS diagram (see Figure 2), with values in the ranges 14–14.5 °C and 38.6–38.8 psu, respectively. The TIW is present in most of the TYS, and originates from local winter convection processes [21–23]. It has similar characteristics to those of the Western Intermediate Water (WIW), which is formed in winter in the Liguro-Provençal and Algerian basins. Winter convection in the TYS is particularly strong in the area of the Bonifacio cyclone, where the mixing induces a homogenization of the water column until a depth of about 400 m.

As far as the horizontal distribution of the LIW is concerned, three distinct regions can be identified: one, near the Sicily Channel, which is the region with maximum values of salinity, and is characterized by the strong mixing among the LIW, inflowing through the channel sills, and less dense local waters (e.g., [24]); a central region, in which horizontal exchanges are prevalent; and the northern region, where, as for the surface waters, strong vertical mixing takes place, strongly reducing the local values of salinity.

2.2. Deep Waters

Below 1000–1500 m there is the WMDW, which is formed during the processes of deep convection in the Gulf of Lion, and more generally in the Liguro-Provençal basin, and enters the TYS after crossing the Sardinia Channel. Between the LIW and the WMDW there is the TDW [22,25], a local water mass resulting from the mixing of the LIW with resident deep water, which is characterized by a relative minimum of dissolved oxygen, and has temperature and salinity slightly higher (by about 0.2 °C and 0.03 psu) than those of the WMDW. This water is exported into the western part of the western Mediterranean through the Sardinia Channel.

An important feature of the TYS deep waters is represented by the staircase structures that are observed in the temperature and salinity profiles (see, e.g., Figure 1 of [26]). These structures are typical of the transition region between LIW and deep water (e.g., [26,27]), and result from phenomena of double diffusion. Double diffusion in the ocean is a convective overturning motion driven by the difference in magnitude between the molecular diffusion coefficients for heat and salt, which depends on the vertical gradients of temperature and salinity. When both gradients are positive (warm and salty water overlying colder and fresher), it is called “salt finger convection”, and this is typically the phenomenon occurring in the Tyrrhenian Sea.

3. Surface Circulation

The description of the Tyrrhenian water masses of the previous section has also highlighted the complexity of the exchanges occurring through the three main openings of the TYS. These are sometimes associated to robust, spatially well-defined currents, which, together with the atmospheric forcing at the air-sea interface, play a key role in determining the structure of the surface circulation. One of these currents is the strong AW surface stream that, after following the African coastline, crosses the southern part of the Sardinia Channel and bifurcates twice before reaching Sicily (see the path schematically indicated by the red arrows in Figure 1). Two branches cross the Sicily Strait, the so-called Atlantic Tunisian Current and Atlantic Ionian Stream (see [28,29], a recent study of the circulation variability in the region), whereas the remaining current, from late autumn to the beginning of spring, enters the TYS. The latter stream then makes a wide cyclonic path along the Sicilian and Italian coasts, and finally outflows into the Ligurian Sea through the Corsica Channel; only a small fraction of it recirculates towards the south, exiting through the northern part of the Sardinia Channel. The results of [30] indicate that in winter 2004, the transport associated to the current entering from the Sardinia Channel was of about 2 Sv, whereas that associated to the branch that enters the TYS and then exits at Corsica was of about 1 Sv. The latter is also a typical average winter value of the transport through the Corsica Channel, estimated from the current measurements performed since 1985 at a mooring in the sill of the channel [31,32].

As shown in [10,33], a more detailed picture of the TYS surface circulation can be obtained from the analysis of altimeter maps (produced by AVISO, and now distributed by CMEMS), which have a spatial resolution of $1/8^\circ$ (about 14 km) over the Mediterranean Sea (twice the detail of the maps for the global ocean). The merged and delayed maps are particularly useful, because they result from the off-line elaboration of data from all the available tracks. We have used these maps, which now have daily frequency, to produce seasonal means of the ADT for winter and summer, averaged over 25 years (1993–2017). These average maps, shown in Figure 3, are similar, but not identical, to analogous maps displayed in Figure 4 of [10], obtained using an older version of the altimeter dataset, covering a shorter period. In Figure 3, colours denote the ADT values, and geostrophic reconstructions of the circulation, also provided by AVISO, have been superimposed to the ADT maps. The dark dot in the south-eastern part of the basin, centred at (39.48°N , 14.82°E), approximately corresponds to the highest portion of the central edifice of the Palinuro Seamount, which is the most extended and taller, with a summit at about 80 m from the sea surface (see [34,35] for a detailed description of the bathymetry in the area). We recall that the Palinuro volcanic system is oriented almost zonally, and extends for more than $1/2^\circ$ in longitude and about $1/4^\circ$ in latitude.

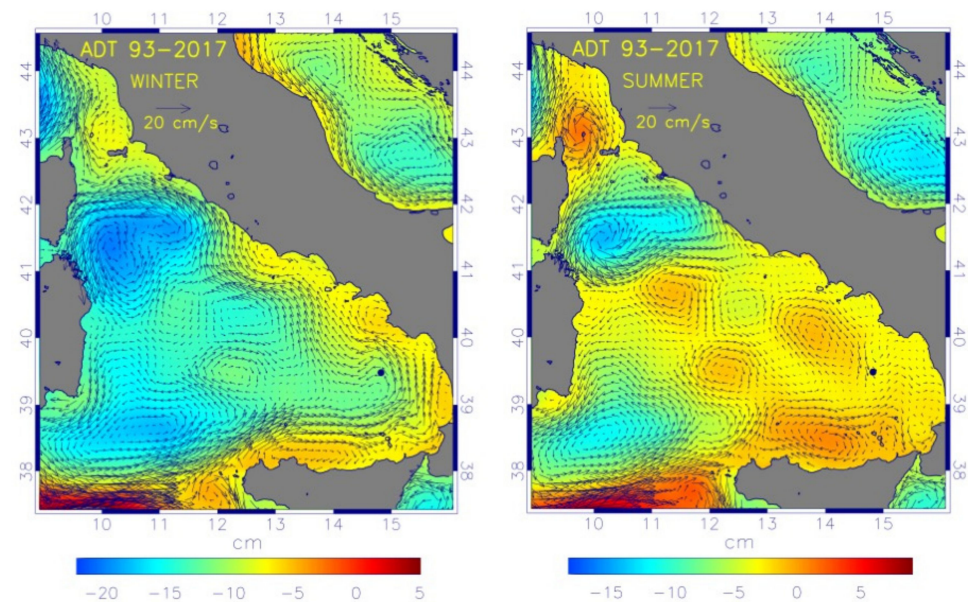


Figure 3. Average ADT maps (1993–2017) over the Tyrrhenian Sea, for winter (left) and summer (right), with the associated geostrophic circulations superimposed. The dark dot in the south-eastern part of the basin marks the location of the central edifice of the Palinuro Seamount.

3.1. Seasonal Variability

The permanent circulation structures in the western TYS, schematically indicated by yellow ovals in Figure 1, are readily recognized in the maps of Figure 3. To the north is the Bonifacio dipole [11,36], driven by the year-long westerly winds blowing over the Bonifacio Strait. To the south, a wide cyclonic area between Sardinia and Sicily, already present in the circulation schemes of Krivosheya [6], summarizing the results of Russian experimental campaigns of the preceding decades. In winter, these structures are inserted in a global cyclonic cell that is sustained by wind-forcing, which is cyclonic over most of the basin. The surface current previously described, circulating along the Sicilian and Italian coasts, forms meanders that indicate the presence of an instability [10]. In the transition between winter and spring, this leads to the formation of anticyclones along the coast and cyclones on the offshore side of the current, similarly to what has been observed in other regions of the Mediterranean, such as the Algerian basin (see, e.g., [37,38], where the evolution of anticyclonic eddies forming between the AW current and the Algerian coast is analysed).

One of the meanders is in the area of the Palinuro Seamount, with the current apparently turning cyclonically around the central edifice of the volcano. Considering the dimensions of the latter, and the proximity of its summit to the sea surface, it cannot be excluded that the geostrophic reconstruction of the circulation is here capturing an effect related to the presence of the seamount. Analogous flow patterns in the area are present in the maps of the circulation at a depth of 10 m (March 2009) shown in Figure 8 of [10]. These maps, which illustrate the development of the instability, derive from the outputs of a high-resolution (horizontal grid spacing of about 2 km) numerical model of the TYS circulation.

The map on the right in Figure 3 shows that the summer circulation is quite different from the winter one. The region between the northern end of Corsica and the Elba Island is now occupied by an anticyclone, denoted as the Ligurian anticyclone in [19], which appears to separate the TYS circulation from that of the Ligurian Sea (see [2], and references therein). This is consistent with the fact that the observed transports through the Corsica Channel are typically very small in summer.

At the same time, in the southern TYS, the AW stream coming from the Sardinia Channel only feeds the branches veering towards the Levantine basin, while very little flow appears to enter the eastern TYS, which remains basically isolated. This allows the anticyclonic eddies formed near the coast in spring to grow, becoming dominant elements of the local circulation, also sustained by the strengthening of the negative wind-stress curl pole present to the north of Sicily [10]. One of these structures is located in front of the Campania region, and extends until the Palinuro Seamount, which, together with the adjacent Marsili Seamount, also appears to have a direct effect on the circulation in this case, delimitating the extension of the cell towards the southeast.

To conclude this description of seasonality, we may briefly highlight the effects of the surface circulation on the spatial distribution of the tracers, and particularly of the salinity. Figure 5.11 of [39] shows the distribution of the minimum of salinity in winter and summer, obtained from high-resolution simulations of the TYS circulation. In winter (left panel), the lowest values of the salinity minimum inside the TYS are in the region interested by the AW current that circulates along the Italian coasts, and slowly increase along the path of the current, indicating that the AW is not subject to strong mixing along this path. On the other hand, much higher values are found in the western part of the TYS, where the presence of the cyclonic circulations induces vigorous mixing with the intermediate waters [7,21,39]. In summer, minimum values of salinity are found in the whole eastern part of the basin, where no strong current is present. These numerical findings are consistent with the picture previously developed from the observations [7].

3.2. Coastal Dynamics in the Central TYS

Since the Palinuro Seamount is not far from the Italian coast and, in particular, from the coasts of Campania, it is natural to wonder whether this area has been included in some regional studies of coastal circulation. The answer appears to be negative, but the circulation along the Campania coasts has attracted considerable attention in the last decade. Of course, the hotspot in the area is represented by the Gulf of Naples, because of the local, intense socio-economic activities; the dynamics and the ecosystems in the area have been monitored and studied for a long time (see the review [40]). The variability of the circulation in the Campania coastal area, which includes the Gulf of Naples, together with the Gulf of Gaeta (to the north) and that of Salerno (to the south), has been investigated in [41] (see also references therein), using a very high-resolution numerical model, nested with a TYS circulation model. An important point emerging from this work is that, besides the atmospheric forcing, the interaction with the offshore circulation also plays an important role in shaping the local dynamics. The circulation in the three gulfs is mostly controlled by the local wind stress in autumn and winter, whereas the interaction with the offshore large-scale circulation and baroclinic effects related to topographic variations are important during spring and summer.

Unfortunately, the area of the Palinuro and Marsili Seamounts is out of the computational domain of these works, more to the southeast, and is likewise not reached by the experimental transect, going from the Gulf of Naples to a central location of the TYS, along which repeated hydrological measurements have been collected during the VECTOR Project [42]. Information on the circulation in the area could, in principle, be obtained from the analysis of the outputs of the Mediterranean Sea circulation forecast model available through CMEMS, but no such study appears to have been conducted so far.

4. Intermediate and Deep Circulation

Until the beginning of the present century, knowledge about the intermediate and deep circulations of the TYS was mostly based on hydrological observations (see [9]), and on the current measurements at the straits. More recently, a description of the intermediate circulation of the Mediterranean Sea based on the analysis of Argo drifter data has been proposed in [43], but as far as the TYS is concerned, this description appears similar to the picture that had previously been drawn, in which the large-scale intermediate circulation is basically characterized by a cyclonic path along the coasts of the basin (see, e.g., the scheme in Figure 3 of [9]). As a matter of fact, the path of the LIW inside the TYS has been unclear for long time. One of the rare dedicated experimental works that has contributed to its clarification is [44], in which measurements from cruises performed between February 1988 and August 1990 were analysed. In that work, evidence was found of the presence of a LIW current flowing anticlockwise along the coasts of Latium (central Italy), at depths between 250 and 700 m, particularly strong in winter. The signature of this current, as a local maximum in salinity, has also been found more to the south, along the VECTOR transect [42]. The presence of LIW in the outer portion of the Gulf of Naples has been known for decades [45].

A weak, and not well-structured LIW average flow (between 200 and 300 m) was found in the re-analysis of the Mediterranean circulation discussed in [46]. Marked seasonal variations were instead highlighted in [39], analysing the 2009 circulation patterns from a high-resolution operational forecast model of the TYS. We have performed a similar analysis using forecasts produced by the MITO model (forecasts can be found on the website <https://giotto.casaccia.enea.it/mito/> (accessed on 16 April 2021)), a recently developed, high-resolution, tide-including operational model of the whole Mediterranean Sea—Black Sea system [47]. The panels in Figure 4 display the average currents at 300 m, for March and September 2020, obtained from the MITO forecasts.

The March current patterns are similar to those for February 2009 shown in [39], with a robust stream of LIW that enters the TYS from the Sicily Channel, and then veers towards the east, proceeding cyclonically all along the Italian continental shelf, until the Corsica Channel. The structure of the circulation has strong similarities with that of the surface winter circulation produced by the model (not shown), with the main large mesoscale features (e.g., the Bonifacio dipole, and the cyclonic circulation to the south of it) present in both layers, indicating the presence of a robust barotropic component of the basin dynamics, similarly to what was found in [39]. It can be noted that a fraction of the LIW current entering from the Sicily Channel appears to be entrapped in the wide cyclonic area between Sardinia and Sicily, and slowly transported towards the Sardinia Channel. The September circulation map is characterized by a much more direct LIW path towards the northwest, heading for the Sardinia Channel; the LIW cannot penetrate in the southeastern part of the TYS, where a wide anticyclonic circulation is present, similarly to what happens in the surface layer.

This strong difference between the winter and summer intermediate circulations is further highlighted in Figure 7 of [39], displaying the spatial distributions of the salinity maximum over the water column obtained from the model, for February and September 2009.

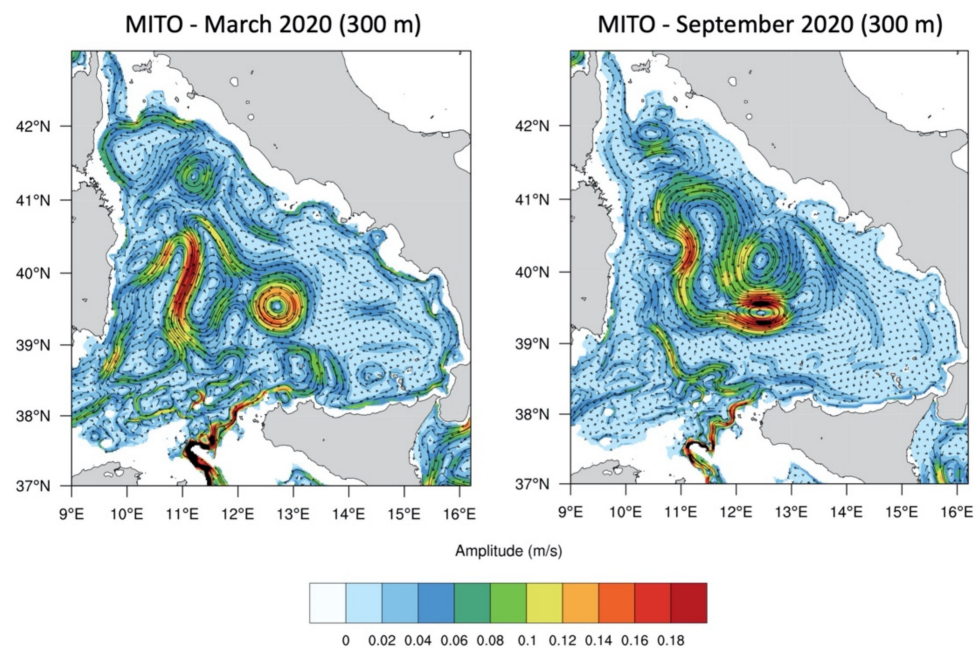


Figure 4. Intermediate TYS circulation (300 m of depth) for March and September 2020, from MITO forecasts (see the text for details).

By contrast, little is known about the deep circulation (below 1000 m) of the TYS, except for the fact that it should be mainly determined by the transport of WMDW coming from the Algerian basin through the Sardinia Channel. In the absence of direct current measurements, hypotheses have been formulated [8] based on hydrological observations, which lead to a scheme of the deep circulation similar to that for the intermediate circulation, characterized by a cyclonic path along the coasts of the basin, controlled by the topography. Recent work [48] indicates that bottom currents may have an important role in shaping the spatial distribution of bottom sediments and microplastics in the northern TYS.

We finally recall that the first description of the deep circulation in the western part of the western Mediterranean Sea has recently been provided in [49]. This study, based on the analysis of data from profiling floats drifting at depths of 1200 and 1900 m for the period 1997–2002, revealed a rich dynamical structure that still has uncertainties, but can be considered as a first step in the characterization of deep circulation processes in this portion of the Mediterranean basin.

5. Long-Term Variability

Variability of the circulation also takes place on scales longer than the seasonal one. Variations on scales of a few years have been observed, which may be related to the variability of the atmospheric forcing. An example is the modulation of the winter transport through the Corsica Channel highlighted in [32], which was shown to be correlated with the North Atlantic Oscillation (NAO; see [50]). Another example was given in [10], where a nonlinear spectral analysis [51] of the altimeter data over the TYS revealed that, besides the dominant seasonal mode, a significant low-frequency mode of variability was also present. This mode has a period of about six years, and is mostly localized in the western part of the basin, but its origin has not yet been clarified.

Longer-term variations may be induced by climate change, and are now well-documented, both on global (see, e.g., the SST warming trend highlighted in the Fifth Assessment Report of the IPCC; [52]) and regional scales. These changes are significant in the Mediterranean Sea ([53,54], among others), even though the estimated trends of surface temperature may vary with the period, geographical area, and methodology considered; recent works on the warming of the Mediterranean SST are [3,17,55]. The rising SSTs appear to influence the weather and to amplify the magnitude and frequency of extreme events (e.g., [56]), with

potentially important impacts on communities and ecosystems, particularly in sub-basins, such as the TYS, with a very high population density in the coastal areas.

In a recent work focusing on the TYS [57], 37 years (1982–2018) of satellite-derived data were used to investigate the SST variability in relation to large-scale and local forcing mechanisms. The TYS SST linear warming trend found in this work, 0.034 ± 0.004 °C/year (which gives a warming of 1.288 ± 0.129 °C through the considered period), is not very different from the Mediterranean trends found in other works (e.g., the trend of 0.036 ± 0.003 °C/year obtained in [17], for the period 1993–2017). However, it was argued in [57] that the trend appears to vary throughout the almost four decades examined, and that this variability may be associated to that of some global atmospheric patterns (see also the references in [57], about the role of teleconnections).

In the last few decades, another important source of long-term variability in the Mediterranean Sea was represented by the Eastern Mediterranean Transient (EMT), a dramatic event which occurred at the beginning of the 1990s (see [58–60], among others). This generated a strong anomaly in the production of intermediate and deep waters in the Eastern Mediterranean, whose effects have subsequently “propagated” throughout the whole Mediterranean basin. Thanks to the large amount of data collected over the last few decades, it has been possible to track the evolution of the water mass characteristics under the influence of the transient. An example is the increase of density in the Sicily westward outflow that produced a cascade of warm and salty water in the deep TYS during the 1990s [61]. In [62], two main phases of the EMT were identified in the TYS, a “deep” and an “intermediate” one, using the time-series of temperature at 400 m and 1800 m, from the mid-1980s to mid-2000s. The deep phase was marked by an increase of temperature in the deep central basin (at 1800 m depth; see their Figure 4a), starting from 1992, which resulted from the sinking of the denser Sicily outflow. This increase lasted until 2001, and the propagation of this signal outside the Tyrrhenian Sea contributed to an enhancement of positive salt and heat trends in the Ligurian Sea, during 1995–2004. The (subsequent) intermediate phase was instead identified from the temporal evolution of the temperature in the LIW layer (at 400 m depth, their Figure 4b), with a temperature increase (representative of the EMT signal) observed at the Corsica Channel and then in the Ligurian Sea after 2001, and somewhat later in the central TYS. It was suggested that this apparently counterintuitive result could be explained by the presence of the fast boundary current flowing around the Italian coast we have been discussing in the previous Section. On the other hand, an increase in salinity at the Sardinia Channel has apparently been observed only from the end of 2004 (an increase from 38.65 during the 1990s up to 38.7 in 2004–2005).

A recent warming of the LIW in the TYS was also documented in [63], which is based on the analysis of XBT data from the period 1999–2014. In 2014, the LIW layer was found to be anomalously warm, similarly to what observed in 2004, and it was consequently argued that these warmings could be related to EMT-like events, since the LIW may take about 10 years to go from the Levantine basin to the Sicily Channel (e.g., [64]). It has then been shown in [21] that the LIW warming has continued in 2015 and 2016, and that in the period 2014–2016 there has also been a warming of the TIW, but with a significantly stronger rate, indicating that part of the TIW warming may result from the warming of the surface layer on a Mediterranean Sea scale.

We finally recall that, according to [4], the basic structure of the intermediate and deep layers of the WMED has abruptly changed since 2005; analysis of a large number of hydrological observations has provided evidence of reinforced thermohaline variability in the deep western basin, with significant dense water-formation events producing large amounts of warmer, saltier and denser water masses than ever before.

It is worth nothing that the warming and saltening of the Mediterranean observed in the last few decades may be an expression of a climate change that will continue in the future. According to the scenario simulations analysed in Adloff et al. [65], a comparison of the 2070–2099 period with 1961–1990 shows that the sea surface temperature

anomalies range from +1.73 to +2.97 °C and the SSS anomalies spread from +0.48 to +0.89. The numerical experiments suggest the choice of the near-Atlantic surface water evolution has the largest impact on the evolution of the Mediterranean water masses.

6. Seamount Effects

Since seamounts play an important role in the Marine Hazard Project, to which this special number of Sustainability is dedicated, it seems appropriate to highlight some effects that such structures may have on the circulation, and recall some works that have focused on Tyrrhenian seamounts.

The numerous isolated topographic structures that characterize the TYS bathymetry result from a complicated morphogenesis, whose principal phases are summarized, for example, in [66]. A precious reference in this context is the “Atlas of the Mediterranean Seamounts and Seamount-like Structures” [67], published in 2015 by the International Union for Conservation of Nature and Natural Resources (IUCN). Many Tyrrhenian seamounts are classified and described in the Atlas; for each of them, there is a short description of the geological context, and, where available, details about observations, with a focus on biological aspects.

The large number of TYS seamounts in the Atlas is due to the very complex bathymetry of the basin, but also to the choice of considering any elevation rising at least 100 m from the surrounding seafloor as a seamount. The authors point out that there are many possible—and used—definitions of seamount, and that the choice of 100 m as a lower cut-off, instead of larger values used in the past, is in line with the more recent literature. For many of the Tyrrhenian seamounts, however, the distance of the peaks from the surrounding seafloor is of several hundred meters, and it is close to 1000 and even larger for some of them (Marsili, Vercelli, Vavilov, Palinuro, among others). Some rise almost to the sea surface, with peaks at less than 100 m of depth (e.g., Vercelli and Palinuro).

These isolated topographic features may have effects on the surrounding circulation that are briefly recalled in the introduction of [68], a very recent work focusing on dynamical and biological features in the area of the Senghor Seamount, a shallow Atlantic seamount, located to the northeast of the Cape Verde Archipelago. Besides quasi-steady effects, such as the creation of Taylor caps (e.g., [69]) and the deflection of currents, there may be enhanced turbulent mixing [70], upwelling or downwelling along the seamount flanks, trapping of tidally generated internal waves [71], and strong interactions with propagating eddies (see [72], and references therein), among other features (see the bibliography in [68]).

Few investigations of dynamical effects connected with Tyrrhenian seamounts have apparently been performed. In [73], an anticyclonic eddy observed in July and December 2005 in a central region of the TYS was analyzed, and it was suggested that the persistence of this vortex could be associated to the presence of the Vavilov Seamount nearby. The presence of the anticyclone was found to be associated with positive anomalies in the SLA (sea level anomaly; the quantity actually measured from satellite altimeters) in the area of the seamount, which were also present a few other times during the period 1993–2006. The presence of this vortex was further discussed in [19], where it was noted that the structure could not always be found in XBT data. This suggests that its persistence in the ADT maps (see Figure 3, in the box 12° E–13° E, 39° N–40° N) is probably partly due to the presence of an anticyclonic signal in the reconstruction of the mean dynamic topography (MDT, the signal representative of the average circulation that is added to the SLA to produce the ADT; see [74]). We note that a strong anticyclone, in the same area, is also present in the maps of intermediate circulation of Figure 4, extracted from the MITO forecasts. This may be partly due to the fact that the model is initialized once a week with the circulation of a model that assimilates altimeter data, but interaction with the isolated topographic feature cannot be a priori excluded.

A big TYS seamount with its top in the euphotic zone is the Vercelli, in the northern TYS, just above 41° N. An investigation of the effects of this seamount on the surrounding ecosystems and circulation was carried out in [75]. Complex hydrodynamic features were

found, with interesting biological consequences, including an accumulation of nutrients on the summit of the volcano, and the presence of downstream fluxes of nutrients on its NW side. The circulation around the seamount was further investigated in [76], using glider measurements performed in the same experimental campaign of 2009 (Tyrrhenian Seamounts ecosystems: an Integrated Study; TySEc).

Recent work [77] has analyzed the role of geothermal heating sources, which can be present on the flanks of submerged volcanos. It was shown in [77] that the heating can control the dissipation of turbulent kinetic energy and of diapycnal mixing, and can also create thermohaline gradients that can influence the local dynamics.

7. Conclusions

In this review, we have highlighted the complexity of the TYS circulation, which is both determined by local atmospheric forcing and local processes, and by the exchanges with the neighbouring basins. Because of these exchanges, and of its central location inside the Mediterranean, the TYS also reflects the variability of the Mediterranean Sea as a whole, which, as we have seen, has been significant in the last few decades.

Focusing on recent results, we have described some interesting features of the dynamics in the eastern part of the basin, in which the Palinuro Seamount is located. First of all is the presence of a strong seasonality of the circulation in the surface layer. In winter, the area is interested by a strong north-westward current of AW, whereas in summer a wide anticyclonic region is present off the Campania coasts, which appears to be delimited towards the southeast by the Palinuro and Marsili Seamounts. In both cases, one could expect the presence of dynamical interactions with these isolated topographic features. The picture of the intermediate circulation deriving from the observations and recent numerical studies is similar, indicating the presence of a strong barotropic component in the basin dynamics. On the other hand, little is known, at present, about the structure of the deep circulation; we can only wait for an analysis of the deep drifters' measurements that have been made in the last decade, similar to that performed in [49] for the westernmost portion of the western Mediterranean.

In the last decade, the progresses in the numerical simulation of the Mediterranean and TYS circulation have also prompted the first high-resolution numerical investigations of the circulation in coastal regions, particularly in the central part of the basin (Campania coasts). This is something that will probably strongly develop in the near future, following further improvements of the basin scale models (higher spatial resolution, inclusion of the tidal forcing, such as in [47], and so on), and of the observation techniques (e.g., glider observations [78], techniques for improving the quality of altimeter observations near the coast, and the development of new satellite programs). The study of the dynamics in the coastal areas, including high-frequency phenomena that have begun to be investigated (see, e.g., [79]) is of course strongly motivated by the need of mitigating the pressure on the local ecosystems that derives from the growing economic activities exploiting the coastal seas.

The understanding of the seasonal variability of the surface and intermediate circulation is still incomplete. As shown in [10], the surface dynamics in spring and autumn are more complex and difficult to analyse; significant interactions between the bathymetry and the mesoscale structures can be expected, which will need to be investigated. Little is known about the interannual variability; the results of [10], concerning the existence of a low-frequency mode with a period of about six years need to be confirmed, taking advantage of the longer series of observations now available, and the causes of this variability need to be clarified.

In the last decade, a few works have explored "seamount effects" in the TYS, both on the circulation and on the local ecosystems. This is also an area in which significant development is needed and foreseen. We can recall here that 10 years ago, in the conclusions of [30], the possible role that the big, submerged volcanos may have in shaping the mesoscale circulation in the surface and intermediate layers of the eastern TYS was clearly highlighted. It is now time to tackle this difficult problem, using the most recent numerical

instruments that have been developed, to understand the interactions that take place in these layers, and to have a first look at what happens in the deeper regions.

Author Contributions: All authors have contributed to the design of this review and to the writing of the draft. R.I. has coordinated the work, and produced the final manuscript. All authors have read and agreed to the published version of the manuscript.

Funding: This research was funded by the Marine Hazard Project (funds from PON, “Programma Operativo Nazionale” of the Italian Ministry of Education, University, and Research).

Data Availability Statement: Argo data used to construct Figure 2 were obtained from the web site <https://argo.ucsd.edu/data/> (accessed on 16 April 2021), whereas data from altimetric observations used to construct Figure 3 were obtained from the Copernicus Marine Service (<https://marine.copernicus.eu> (accessed on 16 April 2021)). In both cases, data are freely provided for scientific use.

Acknowledgments: The authors thank the three Reviewers for useful comments and suggestions.

Conflicts of Interest: The authors declare no conflict of interest.

References

1. Fossi, M.C.; Romeo, T.; Bains, M.; Panti, C.; Marsili, L.; Campani, T.; Canese, S.; Galgani, F.; Druon, J.N.; Airoidi, S.; et al. Plastic debris occurrence, convergence areas and fin whales feeding ground in the Mediterranean marine protected area Pelagos Sanctuary: A modeling approach. *Front. Mar. Sci.* **2017**, *4*. [CrossRef]
2. Iacono, R.; Napolitano, E. Aspects of the summer circulation in the eastern Ligurian Sea. *Deep Sea Res. Part I* **2020**, *166*, 103407. [CrossRef]
3. Pisano, A.; Marullo, S.; Artale, V.; Falcini, F.; Yang, C.; Leonelli, F.E.; Santoleri, R.; Buongiorno, N.B. New evidence of Mediterranean climate change and variability from sea surface temperature observations. *Remote Sens.* **2020**, *12*, 132. [CrossRef]
4. Schroeder, K.; Chiggiato, J.; Bryden, H.L.; Borghini, M.; Ismail, S.B. Abrupt climate shift in the Western Mediterranean Sea. *Sci. Rep.* **2016**, *6*, 23009. [CrossRef] [PubMed]
5. Monecke, T.; Petersen, S.; Augustin, N.; Hannington, M. Seafloor hydrothermal systems and associated mineral deposits of the Tyrrhenian Sea. *Mem. Descr. Carta Geol. Ital.* **2019**, *104*, 41–74.
6. Krivosheya, V.G. Water circulation and structure in the Tyrrhenian Sea. *Oceanology* **1983**, *23*, 166–171.
7. Astraldi, M.; Gasparini, G.P. The seasonal characteristics of the circulation in the Tyrrhenian Sea. In *Seasonal and Interannual Variability of the Western Mediterranean Sea, Coastal and Estuarine Studies*; Geophysical Monograph Series; La Violette, P., Ed.; American Geophysical Union: Washington, DC, USA, 1994; Volume 46, pp. 115–134.
8. Millot, C. Circulation in the western Mediterranean Sea. *J. Mar. Syst.* **1999**, *20*, 423–442. [CrossRef]
9. Millot, C.; Taupier-Letage, I. Circulation in the Mediterranean Sea. In *The Handbook of Environmental Chemistry*; Springer: Berlin/Heidelberg, Germany, 2005; Volume 5, pp. 29–66.
10. Iacono, R.; Napolitano, E.; Marullo, S.; Artale, V.; Vetrano, A. Seasonal variability of the Tyrrhenian Sea surface geostrophic circulation as assessed by altimeter data. *J. Phys. Oceanogr.* **2013**, *43*, 1710–1732. [CrossRef]
11. Artale, V.; Astraldi, M.; Buffoni, G.; Gasparini, G.P. Seasonal variability of gyre-scale circulation in the Northern Tyrrhenian Sea. *J. Geophys. Res.* **1994**, *99*, 14127–14137. [CrossRef]
12. Pierini, S.; Simioli, A. A wind-driven circulation model for the Tyrrhenian sea area. *J. Mar. Syst.* **1998**, *18*, 161–178. [CrossRef]
13. Roussenov, V.; Stanev, E.; Artale, V.; Pinardi, N. A seasonal model of the Mediterranean Sea general circulation. *J. Geophys. Res.* **1995**, *100*, 13515–13538. [CrossRef]
14. Zavatarelli, M.; Mellor, G.L. A numerical study of the Mediterranean Sea circulation. *J. Phys. Oceanogr.* **1995**, *25*, 1384–1414. [CrossRef]
15. Marullo, S.; Santoleri, R.; Bignami, F. The surface characteristics of the Tyrrhenian Sea: Historical satellite data analysis. In *Seasonal and Interannual Variability of the Western Mediterranean Sea, Coastal and Estuarine Studies*; Geophysical Monograph Series; American Geophysical Union: Washington, DC, USA, 1994; Volume 46, pp. 135–154. [CrossRef]
16. Amitai, Y.; Lehahn, Y.; Lazar, A.; Heifetz, E. Surface circulation of the eastern Mediterranean Levantine basin: Insights from analyzing 14 years of satellite altimetry data. *J. Geophys. Res.* **2010**, *115*, C10058. [CrossRef]
17. Mohamed, B.; Mohamed, A.; El-Din, K.A.; Nagy, H.; Shaltout, M. Inter-annual variability and trends of sea level and sea surface temperature in the Mediterranean Sea over the last 25 years. *Pure Appl. Geophys.* **2019**, *176*, 3787–3810. [CrossRef]
18. Rubino, A.; Gačić, M.; Bensi, M.; Kovacevic, V.; Malačić, V.; Menna, M.; Negretti, M.E.; Sommeria, J.; Zanchettin, D.; Barreto, R.V.; et al. Experimental evidence of long-term oceanic circulation reversals without wind influence in the North Ionian Sea. *Sci. Rep.* **2020**, *10*, 1905. [CrossRef]
19. Ciuffardi, T.; Napolitano, E.; Iacono, R.; Reseghetti, F.; Raiteri, G.; Bordone, A. Analysis of surface circulation structures along a frequently repeated XBT transect crossing the Ligurian and Tyrrhenian seas. *Ocean Dyn.* **2016**, *66*, 767–783. [CrossRef]
20. Poulain, P.M.; Menna, M.; Gerin, R. Mapping Mediterranean tidal currents with surface drifters. *Deep Sea Res. Part I* **2018**, *138*, 22–33. [CrossRef]

21. Napolitano, E.; Iacono, R.; Ciuffardi, T.; Reseghetti, F.; Poulain, P.M.; Notarstefano, G. The Tyrrhenian intermediate water (TIW): Characterization and formation mechanisms. *Prog. Oceanogr.* **2019**, *170*, 53–68. [[CrossRef](#)]
22. Hopkins, T.S. Recent observation on the intermediate and deep water circulation in the southern Tyrrhenian Sea. In *Océanographie Pélagique Méditerranéenne*; Oceanologica Acta; Special Issue; Minas, H.-J., Nival, P., Eds.; Archimer: Copenhagen, Denmark, 1988; pp. 41–50. Available online: <https://archimer.ifremer.fr/doc/00267/37839/> (accessed on 12 May 2019).
23. Povero, P.; Hopkins, T.S.; Fabiano, M. Oxygen and nutrient observations in the Southern Tyrrhenian Sea. *Oceanol. Acta* **1990**, *13*, 299–305.
24. Sparnocchia, S.; Gasparini, G.P.; Astraldi, M.; Borghini, M.; Pistek, P. Dynamics and mixing of the Eastern Mediterranean outflow in the Tyrrhenian basin. *J. Mar. Syst.* **1990**, *20*, 301–317. [[CrossRef](#)]
25. Rhein, M.; Send, U.; Klein, B.; Krhman, G. Interbasin deep water exchange in the western Mediterranean. *J. Geophys. Res.* **1999**, *104*, 23495–23508. [[CrossRef](#)]
26. Durante, S.; Schroeder, K.; Mazzei, L.; Pierini, S.; Borghini, M.; Sparnocchia, S. Permanent thermohaline staircases in the Tyrrhenian Sea. *Geophys. Res. Lett.* **2019**, *46*, 1562–1570. [[CrossRef](#)]
27. Zodiatis, G.; Gasparini, G.P. Thermohaline staircase formations in the Tyrrhenian Sea. *Deep Sea Res. Part I* **1996**, *43*, 655–678. [[CrossRef](#)]
28. Robinson, A.R.; Sellschopp, J.; Warn-Varnas, A.; Leslie, W.G.; Lozano, C.J.; Haley, P.J., Jr.; Anderson, L.A.; Lermusiaux, P.F.J. The Atlantic Ionian stream. *J. Mar. Syst.* **1999**, *20*, 129–156. [[CrossRef](#)]
29. Menna, M.; Poulain, P.M.; Ciani, D.; Doglioli, A.; Notarstefano, G.; Gerin, R.; Rio, M.H.; Santoleri, R.; Gauci, A.; Drago, A. New insights of the Sicily Channel and Southern Tyrrhenian Sea variability. *Water* **2019**, *11*, 1355. [[CrossRef](#)]
30. Vetrano, A.; Napolitano, E.; Iacono, R.; Schroeder, K.; Gasparini, G.P. Tyrrhenian Sea circulation and water mass fluxes in spring 2004: Observations and model results. *J. Geophys. Res.* **2010**, *115*, C06023. [[CrossRef](#)]
31. Astraldi, M.; Balopoulos, S.; Candela, J.; Font, J.; Gacic, M.; Gasparini, G.P.; Manca, B.; Theocaris, A.; Tintore, J. The role of straits and channels in understanding the characteristics of Mediterranean circulation. *Prog. Oceanogr.* **1999**, *44*, 65–108. [[CrossRef](#)]
32. Vignudelli, S.; Gasparini, G.P.; Astraldi, M.; Schiano, M.E. A possible influence of the North Atlantic oscillation on the circulation of the Western Mediterranean Sea. *Geophys. Res. Lett.* **1999**, *26*, 623–626. [[CrossRef](#)]
33. Rinaldi, E.; Nardelli, B.B.; Zambianchi, E.; Santoleri, R.; Poulain, P.M. Lagrangian and Eulerian observations of the surface circulation in the Tyrrhenian Sea. *J. Geophys. Res.* **2010**, *115*, C04024. [[CrossRef](#)]
34. Milano, G.; Passaro, S.; Sprovieri, M. Present-day knowledge on the Palinuro Seamount (south-eastern Tyrrhenian Sea). *Boll. Geofis. Teor. Appl.* **2012**, *53*, 403–416. [[CrossRef](#)]
35. Innangi, S.; Passaro, S.; Tonielli, R.; Milano, G.; Ventura, G.; Tamburrino, S. Seafloor mapping using high-resolution multibeam backscatter: The Palinuro Seamount (Eastern Tyrrhenian Sea). *J. Maps* **2015**. [[CrossRef](#)]
36. Moen, J. *Variability and Mixing of the Surface Layer in the Tyrrhenian Sea*; Milex-80; Technical Report; SAACLANT ASW Research Centre: La Spezia, Italy, 1984.
37. Puillat, I.; Taupier-Letage, I.; Millot, C. Algerian eddies lifetime can near 3 years. *J. Mar. Syst.* **2002**, *31*, 245–259. [[CrossRef](#)]
38. Pessini, F.; Cotroneo, Y.; Olita, A.; Sorgente, R.; Ribotti, A.; Jendersied, S.; Perilli, A. Life history of an anticyclonic eddy in the Algerian basin from altimetry data, tracking algorithm and In Situ observations. *J. Mar. Syst.* **2020**, *207*, 103346. [[CrossRef](#)]
39. Napolitano, E.; Iacono, R.; Marullo, S. The 2009 surface and intermediate circulation of the Tyrrhenian Sea as assessed by an operational model. *Geophys. Monogr. Ser.* **2014**, *202*, 59–74. [[CrossRef](#)]
40. Cianelli, D.; Uttieri, M.; Buonocore, B.; Falco, P.; Zambardino, G.; Zambianchi, E. Dynamics of a very special Mediterranean coastal area: The Gulf of Naples. In *Mediterranean Ecosystems: Dynamics, Management and Conservation*; Williams, S.G., Ed.; Nova Science Publishers, Inc.: Hauppauge, NY, USA, 2012; ISBN 978-1-61209-146-4.
41. De Ruggiero, P.; Esposito, G.; Napolitano, E.; Iacono, R.; Pierini, S.; Zambianchi, E. Modelling the marine circulation of the Campania coastal system (Tyrrhenian Sea) for the year 2016: Analysis of the dynamics. *J. Mar. Syst.* **2020**, *210*, 103388. [[CrossRef](#)]
42. Falco, P.; Trani, M.; Zambianchi, E. Water mass structure and deep mixing processes in the Tyrrhenian Sea: Results from the VECTOR project. *Deep Sea Res. Part I* **2016**, *113*, 7–21. [[CrossRef](#)]
43. Menna, M.; Poulain, P.M. Mediterranean intermediate circulation estimated from Argo data in 2003–2010. *Ocean. Sci.* **2010**, *6*, 331–343. [[CrossRef](#)]
44. Serraval, R.; Cristofalo, G.C. On the presence of a coastal current of Levantine intermediate water in the central Tyrrhenian Sea. *Oceanol. Acta* **1999**, *22*, 281–290. [[CrossRef](#)]
45. Hopkins, T.S.; G.O.N.E.G. The existence of the Levantine intermediate water in the Gulf of Naples. *Rapp. Comm. Int. Mer. Médit* **1977**, *24*, 38–41.
46. Pinardi, N.; Zavatarelli, M.; Adani, M.; Coppini, G.; Fratianni, C.; Oddo, P.; Simoncelli, S.; Tonani, M.; Lyubartsev, V.; Dobricic, S.; et al. Mediterranean Sea large-scale low-frequency ocean variability and water mass formation rates from 1987 to 2007: A retrospective analysis. *Prog. Oceanogr.* **2015**, *132*, 318–332. [[CrossRef](#)]
47. Palma, M.; Iacono, R.; Bargagli, A.; Carillo, A.; Lombardi, E.; Napolitano, E.; Pisacane, G.; Sannino, G.; Struglia, M.V.; Fekete, B.M. Short-term, linear, and non-linear effects of the tides on the surface dynamics in a new, high-resolution model of the Mediterranean Sea circulation. *Ocean Dyn.* **2020**, *70*, 935–963. [[CrossRef](#)]
48. Kane, A.I.; Clare, M.A.; Miramontes, E.; Wogelius, R.; Rothwell, J.J.; Garreau, P.; Pohl, F. Seafloor microplastic hotspots controlled by deep-sea circulation. *Science* **2020**, *368*, 1140–1145. [[CrossRef](#)]

49. Send, U.; Testor, P. Direct observations reveal the deep circulation of the Western Mediterranean Sea. *J. Geophys. Res.* **2017**, *122*, 10091–10098. [[CrossRef](#)]
50. Hurrell, J.W. Decadal trends in the North Atlantic oscillation: Regional temperatures and precipitation. *Science* **1995**, *269*, 676–679. [[CrossRef](#)]
51. Ghil, M.; Allen, M.R.; Dettinger, M.D.; Ide, K.; Kondrashov, D.; Mann, M.E.; Robertson, A.W.; Saunders, A.; Tian, Y.; Varadi, F.; et al. Advanced spectral methods for climatic time series. *Rev. Geophys.* **2002**, *40*, 1003. [[CrossRef](#)]
52. Hartmann, D.L.; Tank, A.M.G.K.; Rusticucci, M.; Alexander, L.V.; Brönnimann, S.; Charabi, Y.A.R.; Dentener, F.J.; Dlugokencky, E.J.; Easterling, D.R.; Kapan, A.; et al. Observations: Atmosphere and surface. In *Climate Change 2013: The Physical Science Basis*; Contribution of Working Group I to the Fifth Assessment Report of the Intergovernmental Panel on Climate Change; Stocker, T.F.D., Qin, G.-K., Plattner, M., Tignor, S.K., Allen, J., Boschung, A., Nauels, Y., Xia, V.B., Miedley, P.M., Eds.; Cambridge University Press: Cambridge, UK, 2014; pp. 159–254. [[CrossRef](#)]
53. Vargas-Yanez, M.; Garcia, M.G.; Salat, J.; Garcia-Martinez, M.C.; Pascual, J.; Moya, F. Warming trends and decadal variability in the Western Mediterranean shelf. *Glob. Planet. Chang.* **2008**, *63*, 177–184. [[CrossRef](#)]
54. Lionello, P.; Scarascia, L. The relation between climate change in the Mediterranean region and global warming. *Reg. Environ. Chang.* **2018**, *18*, 1481–1493. [[CrossRef](#)]
55. Pastor, F.; Valiente, J.A.; Khodayar, S. A warming Mediterranean: 38 years of increasing sea surface temperature. *Remote Sens.* **2020**, *12*, 2687. [[CrossRef](#)]
56. Trenberth, K.; Fasullo, J.; Shepherd, J. Attribution of climate extreme events. *Nat. Clim. Chang.* **2015**, *5*, 725–730. [[CrossRef](#)]
57. Krauzig, N.; Falco, P.; Zambianchi, E. Contrasting surface warming of a marginal basin due to large-scale climatic patterns and local forcing. *Nat. Sci. Rep.* **2020**, *10*, 17648. [[CrossRef](#)]
58. Roether, W.B.; Manca, B.B.; Klein, B.; Bregant, D.; Georgopoulos, D.; Beitzel, V.; Kovačević, V.; Lucchetta, A. Recent changes in eastern Mediterranean deep waters. *Science* **1996**, *271*, 333–335. [[CrossRef](#)]
59. Klein, B.; Roether, W.; Manca, B.B.; Bregant, D.; Beitzel, V.; Kovacevic, V.; Lucchetta, A. The large deep water transient in the Eastern Mediterranean. *Deep Sea Res. Part I* **1999**, *46*, 371–414. [[CrossRef](#)]
60. Theocharis, A.; Klein, B.; Nittis, K.; Roether, W. Evolution and status of the Eastern Mediterranean Transient (1997–1999). *J. Mar. Syst.* **2002**, *33*, 91–116. [[CrossRef](#)]
61. Gasparini, G.P.; Ortona, A.; Budillon, G.; Astraldi, M.; Sansone, E. The effect of the Eastern Mediterranean Transient on the hydrographic characteristics in the Strait of Sicily and in the Tyrrhenian Sea. *Deep Sea Res. Part I* **2005**, *52*, 915–935. [[CrossRef](#)]
62. Shroeder, K.; Gasparini, G.P.; Tangherlini, M.; Astraldi, M. Deep and intermediate water in the western Mediterranean under the influence of the Eastern Mediterranean Transient. *Geophys. Res. Lett.* **2006**, *33*, 21. [[CrossRef](#)]
63. Ribotti, A.; Sorgente, R.; Olita, A.; Orilia, F.; Borghini, M.; Reseghetti, F. Indication of recent warming process at the intermediate level in the Tyrrhenian sea from SOOP XBT measurements. *Mediterr. Mar. Sci.* **2016**, *17*, 467–475. [[CrossRef](#)]
64. Gačić, M.; Schroeder, K.; Civitarese, G.; Cosoli, S.; Vetrano, A.; Borzelli, G.L.E. Salinity in the Sicily Channel corroborates the role of the Adriatic-Ionian Bimodal Oscillating System (BiOS) in shaping the decadal variability of the Mediterranean overturning circulation. *Ocean Sci.* **2013**, *9*, 83–90. [[CrossRef](#)]
65. Adloff, F.; Somot, S.; Sevault, F.; Jordà, G.; Aznar, R.; Déqué, M.; Herrmann, M.; Marcos, M.; Dubois, C.; Padorno, E. Mediterranean Sea response to climate change in an ensemble of twenty first century scenarios. *Clim. Dyn.* **2015**, *45*, 2775–2802. [[CrossRef](#)]
66. Palmiotto, C.; Loreto, M.F. Regional scale morphological pattern of the Tyrrhenian Sea: New insights from EMODnet bathymetry. *Geomorphology* **2019**, *332*, 88–99. [[CrossRef](#)]
67. Würtz, M.; Rovere, M. *Atlas of the Mediterranean Seamounts and Seamount-Like Structures*; IUCN: Gland, Switzerland, 2015; pp. 1–276. [[CrossRef](#)]
68. Mohn, C.; White, M.; Denda, A.; Erofeeva, S.; Springer, B.; Turnewitsch, R.; Christiansen, B. Dynamics of currents and biological scattering layers around Senghor Seamount, a shallow seamount inside a tropical Northeast Atlantic eddy corridor. *Deep Sea Res. Part I* **2021**, *171*, 103497. [[CrossRef](#)]
69. Chapman, D.C.; Haidvogel, D.B. Formation of Taylor caps over a tall and isolated seamount in a stratified ocean. *Geophys. Astrophys. Fluid Dyn.* **1992**, *64*, 31–65. [[CrossRef](#)]
70. Kunze, E.; Toole, J.M. Tidally driven vorticity, diurnal shear, and turbulence atop fieberling seamount. *J. Phys. Oceanogr.* **1997**, *27*, 2663–2693. [[CrossRef](#)]
71. Vlasenko, V.; Stashchuk, N.; Nimmo-Smith, W.A.M. Threedimensional dynamics of baroclinic tides over a seamount. *J. Geophys. Res. Oceans* **2018**, *123*, 1263–1285. [[CrossRef](#)]
72. Sutyrin, G.G. Critical effects of a tall seamount on a drifting vortex. *J. Mar. Res.* **2006**, *64*, 297–317. [[CrossRef](#)]
73. Budillon, G.; Gasparini, G.P.; Shroeder, K. Persistence of an eddy signature in the central Tyrrhenian basin. *Deep Sea Res. Part II* **2009**, *56*, 713–724. [[CrossRef](#)]
74. Rio, M.-H.; Pascual, A.; Poulain, P.M.; Menna, M.; Barcelo', B.; Tintoré, J. Computation of a new mean dynamic topography for the Mediterranean Sea from model outputs, altimeter measurements and oceanographic In Situ data. *Ocean Sci.* **2014**, *10*, 731–744. [[CrossRef](#)]
75. Misic, C.; Bavestrello, G.; Bo, M.; Borghini, M.; Castellano, M.; Harriague, A.C.; Massa, F.; Spotorno, F.; Povero, P. The “seamount effect” as revealed by organic matter dynamics around a shallow seamount in the Tyrrhenian Sea (Vercelli Seamount, western Mediterranean). *Deep Sea Res. Part I* **2012**, *67*, 1–11. [[CrossRef](#)]

-
76. Mauri, E.; Gerin, R.; Poulain, P.M. Glider measurements around the Vercelli Seamount (Tyrrhenian Sea) in May 2009. *Boll. Geofis. Teor. Appl.* **2018**, *59*, 193–202. [[CrossRef](#)]
 77. Ferron, B.; Aubertot, P.B.; Cuypers, Y.; Schroeder, K.; Borghini, M. How important are diapycnal mixing and geothermal heating for the deep circulation of the Western Mediterranean? *Geophys. Res. Lett.* **2017**, *44*, 7845–7854. [[CrossRef](#)]
 78. Aulicino, G.; Cotroneo, Y.; Lacava, T.; Sileo, G.; Fusco, G.; Carlon, R.; Satriano, V.; Pergola, N.; Tramutoli, V.; Budillon, G. Results of the first Wave Glider experiment in the southern Tyrrhenian Sea. *Adv. Oceanogr. Limnol.* **2016**, *7*, 16–35. [[CrossRef](#)]
 79. Martellucci, R.; Pierattini, A.; de Mendoza, F.P.; Melchiorri, C.; Piermattei, V.; Marcelli, M. Physical and biological water column observations during summer sea/land breeze winds in the coastal northern Tyrrhenian Sea. *Water* **2018**, *10*, 1673. [[CrossRef](#)]